International Atomic Energy Agency

INDC(GDR)-044/GI
INT(86)-12

INDC INTERNATIONAL NUCLEAR DATA COMMITTEE

DIFFERENTIAL NEUTRON EMISSION CROSS SECTIONS FROM LEAD AND CARBON BOMBARDED WITH 14 MeV NEUTRONS

T. Elfruth, D. Hermsdorf, H. Kalka, K. Noack, J. Pöthig,
D. Seeliger, K. Seidel and S. Unholzer
Technische Universität Dresden, Sektion Physik,
Mommsenstr. 13, Dresden, DDR-8027, GDR

December 1986

IAEA NUCLEAR DATA SECTION, WAGRAMERSTRASSE 5, A-1400 VIENNA

INDC(GDR)-044/GI
INT(86)-12

DIFFERENTIAL NEUTRON EMISSION CROSS SECTIONS FROM LEAD AND CARBON BOMBARDED WITH 14 MeV NEUTRONS

T. Elfruth, D. Hermsdorf, H. Kalka, K. Noack, J. Pöthig,
D. Seeliger, K. Seidel and S. Unholzer
Technische Universität Dresden, Sektion Physik,
Mommsenstr. 13, Dresden, DDR-8027, GDR

December 1986

Reproduced by the IAEA in Austria
December 1986

87-00197

DIFFERENTIAL NEUTRON EMISSION CROSS SECTIONS FROM LEAD AND CARBON BOMBARDED WITH 14 MEV NEUTRONS

T. Elfruth, D. Hermsdorf, H. Kalka, K. Noack[x], J. Pöthig, D. Seeliger, K. Seidel and S. Unholzer
Technische Universität Dresden, Sektion Physik
Mommsenstr. 13, Dresden, DDR-8027, GDR.

Abstract

Neutron emission cross sections measured with a time-of flight spectrometer which allows accurately to take angular distributions are presented. The date are compared with previous experimental results and with calculations basing on direct, pre-equilibrium and equilibrium emission models.

1. Introduction

Lead is used as neutron multiplier material in conceptual designs of fusion reactors /1/. Therefore, the differential neutron emission cross sections at 14 MeV neutron incidence energy have to be determined with relatively high accuracy /2/. Direct and pre-equilibrium reaction components cause anisotropic, forward-peaked angular distributions, so that the emission spectra must be studied for a wide angular range, especially in their high-energy part. In earlier measurements, spectra were taken only at 90° /3,4/. Later on, angular ranges from 25° to 145° /5/ and from 40° to 150° /6/, respectively, were covered. The low-energy part of the emission spectrum was angle-averaged measured by Vonach et al. /7/. Recently, Takahashi et al. /8/ determined spectra with a high-resolution spectrometer from 15° to 154°.
At the TU Dresden, a time-of-flight (TOF) spectrometer was developed which allows by its arrangement and data acquisition procedure to take spectra from 15° to 165° with widely equal experimental conditions. The spectrometer is described in chapter 2. The obtained data and comparisions with those of previous works are given in chapter 3. A carbon sample was parallely with the lead sample used in the measurements to check spectrometer and data reduction. The obtained data from carbon are also given in chapter 3.

2. Experiment

The geometrical arrangement is shown in Fig. 1. Ring geometry with flight path perpendicularly arranged to the deuteron beam direction, was chosen. The distance between tritium target and neutron detector was 4.9 m. Collimator channel, shadow bar, sample ring and neutron source diameter allowed to measure at scattering angles $15° \leq \vartheta \leq 165°$.

The neutron generator operated in a pulsed regime with deuteron pulses of 2 ns f.w.h.m. and 5 MHz repetition rate /9/, produced

x-Zentralinstitut für Kernforschung, Rossendorf

with a mean deuteron beam of 30 μA a Ti-T-target 2...5x 10^9 neutrons/s. The source strength was determined by counting the α-particles with a silicon surface-barrier detector at $\Phi_0 = 166°$ with respect to the deuteron beam direction. From $dN_\alpha(\Phi_0)/d\Omega$, the neutron production for all directions θ to the deuteron beam $dN_n(\theta)/d\Omega$ was determined calculating $f(\theta, \Phi_0) = \frac{dN_\alpha}{d\Omega}(\Phi_0)/\frac{dN_n}{d\Omega}(\theta)$ for the thick Ti-T-layers of the used targets and measuring the influence of target tube, backing and cooling on the source neutron distribution with $^{27}Al(n,\alpha)$-activation and recoil-proton counting (plastic scintillator, bias at 7 MeV) for the full range of $\theta = 0° ... 180°$. The $f(\theta, \Phi_0)$ corrected for influences of the target construction, were used to calculate for each sample position $f_1(\vartheta, \Phi_0) = \frac{dN_\alpha}{d\Omega}(\Phi_0)/\frac{dN_n}{d\Omega}(\vartheta)$ by averaging over all θ covered by the sample ring. The average neutron incidence energies $E_0(\vartheta)$ were analogously determined. The energy distributions of the neutrons were calculated as functions of θ, and averaging the spectra of those θ covered by the given ring positions resulted in the incidence energy spectra for the ϑ, with their average $E_0(\vartheta)$. $E_0(\vartheta)$ and $f_1(\vartheta, \Phi_0)$ are shown in Fig. 2. Their dependence on ϑ is very weak, since the flight path was arranged at $\theta = 90°$. Furthermore, both functions are symmetric to $\vartheta = 90°$, so that no asymmetries are induced in the neutron emission spectra.

The samples had natural isotopic compositions. The ring had inner diameters of 8.0 cm and outer diameters of 12.0 cm. Their thicknesses in flight-path direction were 1.0 cm for Pb and 1.5 cm for C (pressed powder of density 1.45 g/cm^3) respectively. A ring segment of 4.4 cm width was taken away at the deuteron-beam-tube position in measurements around $\vartheta = 90°$.

The block scheme of the spectrometer is shown in Fig. 3. The neutron TOF detector was a liquid scintillator NE 213 of 12.7 cm in diameter and 3.8 cm length coupled with a XP 2041 photomultiplier. Its anode signals were used for timing as well as for neutron-gamma discrimination /10/ and proton-recoil basing. The neutron detector efficiency $\varepsilon(E)$ was measured by TOF spectrometry of the neutrons emitted from a Cf-252 fission chamber /11/, of the neutons scattered from H replacing the Pb sample in the spectrometer arrangement with a thin polyethylene ring (thickness 0.4 cm) and of the 14 MeV neutrons of the generator removing the shadow bar in the spectrometer.
Besides this measurements, $\varepsilon(E)$ was calculated with the Monte Carlo code NEUCEF /12/. The results are shown in Fig.4 together with the curve used for the data reduction.
The neutron source strength monitored by the α-particle counter was checked during TOF measurements against the counts of two neutron monitors (a plastic scintillation detector with 7 MeV bias and a long counter).
A microcomputer controlled the TOF runs. Sample shifting (ϑ) and changing were free programmable.

Measurements of TOF spectra were carried out for ϑ from 15° to 165° in steps of 15°. In one run, 5 or 6 of these ϑ were chosen symmetrically to $\vartheta = 90°$ and the run was so subdivided in short-time data acquisition periods that the ϑ could be successively covered more than 10 times. The spectra obtained in short-time measurements with and without sample were inspected using the number of events in a given part of the spectrum, the position of the 14 MeV neutron peak and the counts of the monitors and of

Fig. 1
Geometrical arrangement of the time-of-flight spectrometer.
T, tritium target;
S, ring sample;
D, neutron detector.

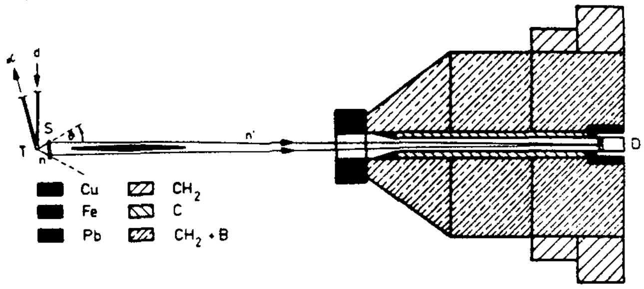

Fig. 2
Average incidence neutron energy (upper part) and number of α-particles/sr counted per neutron/sr (lower part) striking on the sample ring (dashed curves) and on the ring without a segment of 4.4 cm width (solid curves), respectively, as function of the scattering angle.

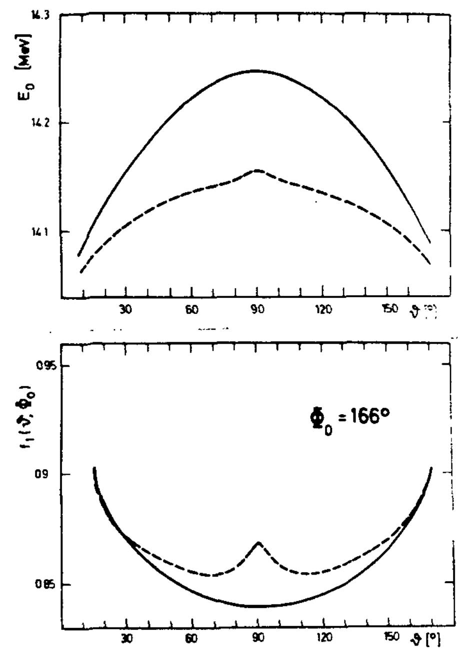

Fig. 3
Block scheme of the spectrometer.
T, tritium target; S, sample;
D, neutron detector;
ZC, zero-crossing trigger;
CF, constant-fraction trigger;
B_n, proton-recoil-energy discriminator; n/γ, neutron-gamma discriminator;
CO, coincidence; ϑ, sample shifter; S, sample changer;
TAC, time-to-amplitude converter; U/D-C, up-and-down counter; ADC, analog-to-digital converter; CC, controller of the CAMAC crate;
MPS, microcomputer.

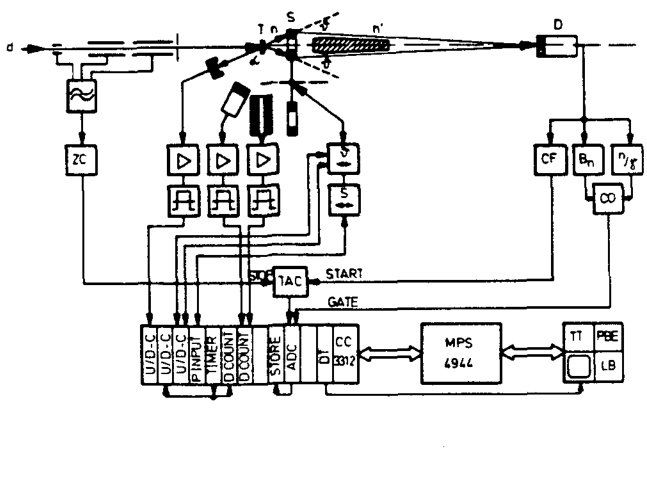

a timer. The spectra were accumulated, if the inspected values were within given intervals. In this way, possible instabilities of the spectrometer or of the generator could be eliminated, and nearly equal experimental conditions, with the exception of the effect/background relation, were realized. Examples of TOF spectra are shown in Ref. /13/. The average width of the time channels was determined with 14 MeV source-neutron TOF peaks shifted by several delay lines in the START branch of the spectrometer. The differential linearity was measured with the statistical events of a Po/Be neutron source.

In the data reduction at first the TOF spectra were corrected for dead time and differential nonlinearity of the spectrometer. Then the effect spectra N(i) were calculated as differences of the spectra obtained with sample and the corresponding taken without sample and taking into account an additional background component determined in the channel region between 14 MeV neutron peak and γ-peak position and assumed to be constant for all channels i. The N(i) were smoothed over about 10 channels with the exception of peak regions. The time scale t was calculated with the average channel width Δt beginning at the peak position of elastically scattered neutrons. The continuous parts of the time spectra $dN(t_i)/dt = N(i)/\Delta t$ were transformed into energy spectra $dN(E_i)/dE$ resulting in laboratory system cross sections by:

$$\sigma_{nm}(E,\vartheta) = \frac{d^2\sigma(E_0;E,\vartheta)}{dE \cdot d\Omega} = \frac{dN/dt \cdot \Delta\Omega_\alpha \cdot L^2 \cdot s^2 \cdot f_1(\vartheta,\phi_0) \cdot f_2(E,\vartheta) \cdot f_3(E,\vartheta)}{N_\alpha \cdot Z_N \cdot F_D \cdot \varepsilon(E)} \quad (1)$$

with N_α being α-counts; $\Delta\Omega_\alpha$, solid angle of α-counting; f_1, number of α-particles/sr counted per neutron/sr striking on the sample; s, distance neutron source/sample; L, distance sample/neutron detector; F_D, neutron detector front-area; ε, neutron detector efficiency; Z_N, number sample nuclei; f_2, correction of multiple scattering in the sample; f_3, correction of flux attenuation in the sample.
The ratio of single-scattered to multiple-scattered neutrons (f_2) was calculated /14/ with the neutron transport code MORSE /15/ using ENDF/B-IV data /16/. The factor f_3^{-1} includes both flux attenuation of the incident neutrons up to the interaction and of the neutrons outgoing in direction of the TOF-detector. It was calculated by integration over the sample volume. The values of $f_2 \cdot f_3$ were between 0.94 and 1.09.
Transformation of the σ_{nm} into center-of-mass system yielded σ_{nm}^{cm}. The formulas used for the data reduction are described in Ref. /17/.

For groups of monoenergetic, scattered neutrons well resolved in dN/dt, the peak areas $N_Q(\vartheta)$ were determined which, replacing dN/dE in eq. (1), yielded $d\sigma(E_0;Q,\vartheta)/d\Omega = \sigma_{nn'}(\vartheta)$. No multiple-scattering correction was carried out for $N_Q(\vartheta)$.

Fig. 4
Neutron detector efficiency measured with TOF spectrometry of 14 MeV source neutrons (□), of neutrons scattered from Hydrogen (Δ) and of Cf-252 fission neutrons (o) and calculated with Monte Carlo technique (-.-). The resulting solid courve was used for the data reduction.

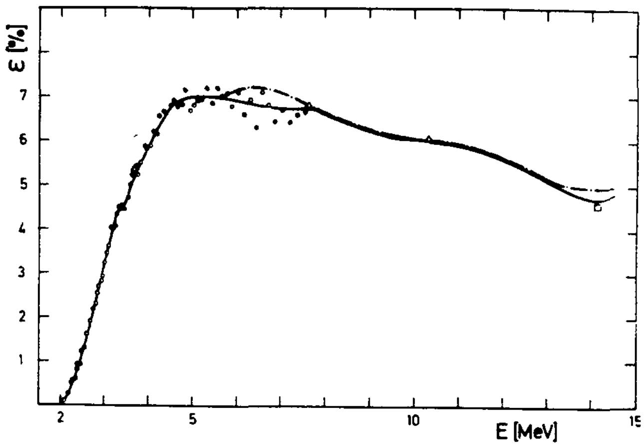

Fig. 5
Angle-integrated emission cross sections of Pb obtained in the present work (o) and compared with experimental data of Hermsdorf et al. (◇,/6/), Vonach et al. (+,/7/) and Takahashi et al. (∇,/8/) and with the ENDF/B-IV evaluation (---).

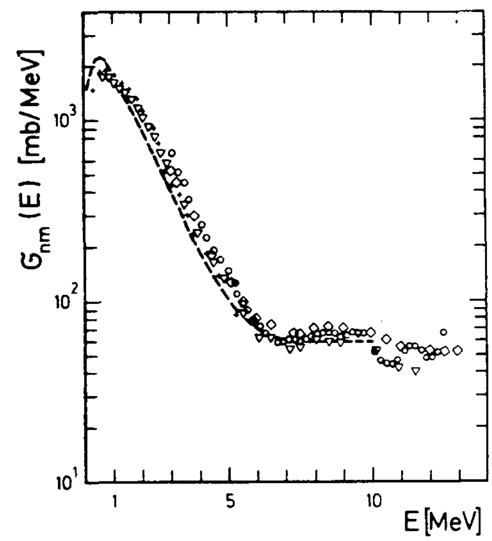

Fig. 6
Measured neutron emission spectrum from Pb (o, present data; ∇,/8/) compared with a theoretical interpretation (——) as direct collective excitations, pre-equilibrium and equilibrium emission of primary neutrons (····) and secondary neutrons from (n,2n).

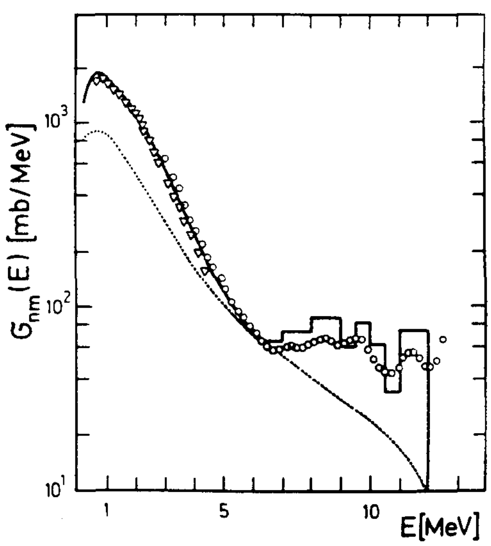

3. Results

The cross sections obtained for Pb are given in Table 1, for C in Table 2. The values $\Delta\sigma/\sigma$ in the tables include only the statistical uncertainties of N(i) or N_{α}, respectively. Systematic uncertainties were estimated to $\Delta\Omega_{\alpha}/\Omega_{\alpha} \lesssim 1$ %, $\Delta L/L \approx 0.4$ %, $\Delta s \lesssim 0.5$ mm, $\Delta f_1/f_1 \approx 2$ %, $\Delta(f_2 \cdot f_3)/(f_2 \cdot f_3) \lesssim 3$ % and $\Delta F_D/F_D \approx 2$ %. The N_{α} had statistical uncertainties which may be neglected but they contained background events which possibly contributed of the order of 1 %. Checks showed that the source-strength monitoring had a total of uncertainties of ≈ 4 %. Calculations of ε(E) with Monte Carlo methods can have uncertainties of ≈ 5 % /18/. Combining the calculation of ε(E) with measured values, $\Delta\varepsilon/\varepsilon$ should be $\lesssim 5$%. The angular resolutions expressed as $\langle\Delta\vartheta^2\rangle^{1/2}$ were $\leq \pm 4^{\circ}$ for Pb and $\leq \pm 5.0^{\circ}$ for C, respectively. The energy resolutions were $\Delta E/E = 3$ % at E = 3 MeV, 5 % at 7 MeV and 7 % at 14 MeV.

For comparisions of the data obtained for Pb with results of other experiments, with theoretical model predictions and with evaluated data, the angle-integrated emission spectrum was derivated,

$$\sigma_{nm}(E) = \frac{d\sigma(E_0;E)}{dE} = \int_{4\pi} d\Omega \cdot \frac{d^2\sigma(E_0;E,\vartheta)}{dE \cdot d\Omega} , \qquad (2)$$

It is plotted in Fig. 5 together was the experimental data of Vonach et al. /7/, of Takahashi et al. /8/ and those of a previous measurement at TU /6/. Taking into account statistical and systematic uncertainties of the data as given by the authors, the four measurements are consistent. Compared with the ENDF/B-IV evaluation the experimentally determined cross sections are obviously larger. Remarkable more neutrons as evaluated are observed in the energy range 1.5 MeV $\leq$ E $\leq$ 5 MeV. The deviation is up to 30 % in the range 2 $\leq$ E $\leq$ 3.5 MeV.
In Fig. 6 the experimental data are theoretically interpreted as superposition of three components: direct excitations of vibrational modes calculated in DWBA approach /19/, pre-equilibrium and compound-nucleus neutron emission calculated with the Generalized Exciton Model code AMAPRE /20/ and secondarily emitted neutrons of (n, 2n) calculated with the statistical model code STAPRE /21/. The agreement of the calculated spectrum with the experimental is satisfactory in the low-energy part. In the high-energy part the neutron emission is overestimated. The direct component with the averaged deformation parameters used would alone explain the neutron emission for E > 8 MeV. But, reducing adequately the pre-equilibrium emission, discrepancies appear in the middle part of the spectrum where only the pre-equilibrium component is able sufficiently to describe the experimental data.

Angular distributions of neutrons emitted from Pb with E = 3.5, 5.5 and 7.5 MeV are presented in Fig. 7. The experimental data show with increasing E a pronounced forward scattering. In the ENDF/B-IV evaluation these angular distributions are assumed to be isotropic. In the measurements of Kammerdiener /5/ and of

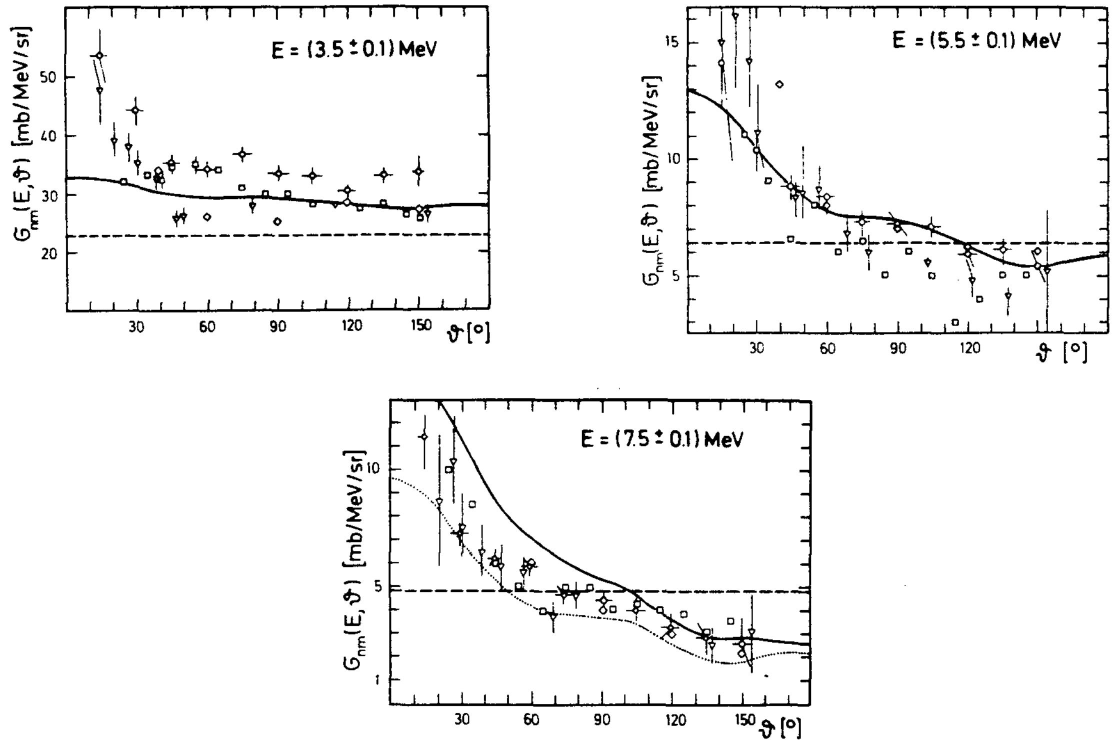

Fig. 7
Angular distributions of neutron emitted from Pb with the energies E inserted. Experimental data (o , present work; x ,/5/; ◊,/6/; ▽,/8/) are compared with the ENDF/B-IV evaluation (---) and with a calculation (——).
The pre-equilibrium and equilibrium component of primary neutron emission (····) is at E = 5.5 MeV practically equal to the total emission (——).

Takahashi et al./8/ the increase of the incidence neutron energy E_0 by about 1.5 MeV going from backward to forward angles has the tendency to overestimate the forward-peaking. The theoretically obtained angular distributions describe the present experimental data at E = 5.5 MeV satisfactory. At E = 3.5 MeV they deviate for $\vartheta \leq 30^{\circ}$ and at E = 7.5 MeV the sum of the calculated direct collective excitations and of the pre-equilibrium emissions overestimates the neutron emission as discussed for the angle-integrated spectrum.

The data obtained for C are compared in Fig. 8 with other experimental data and with the ENDF/B-V evaluation. Generally, they agree with the expected values so that this check of spectrometer and data reduction may be considered to be satisfying.

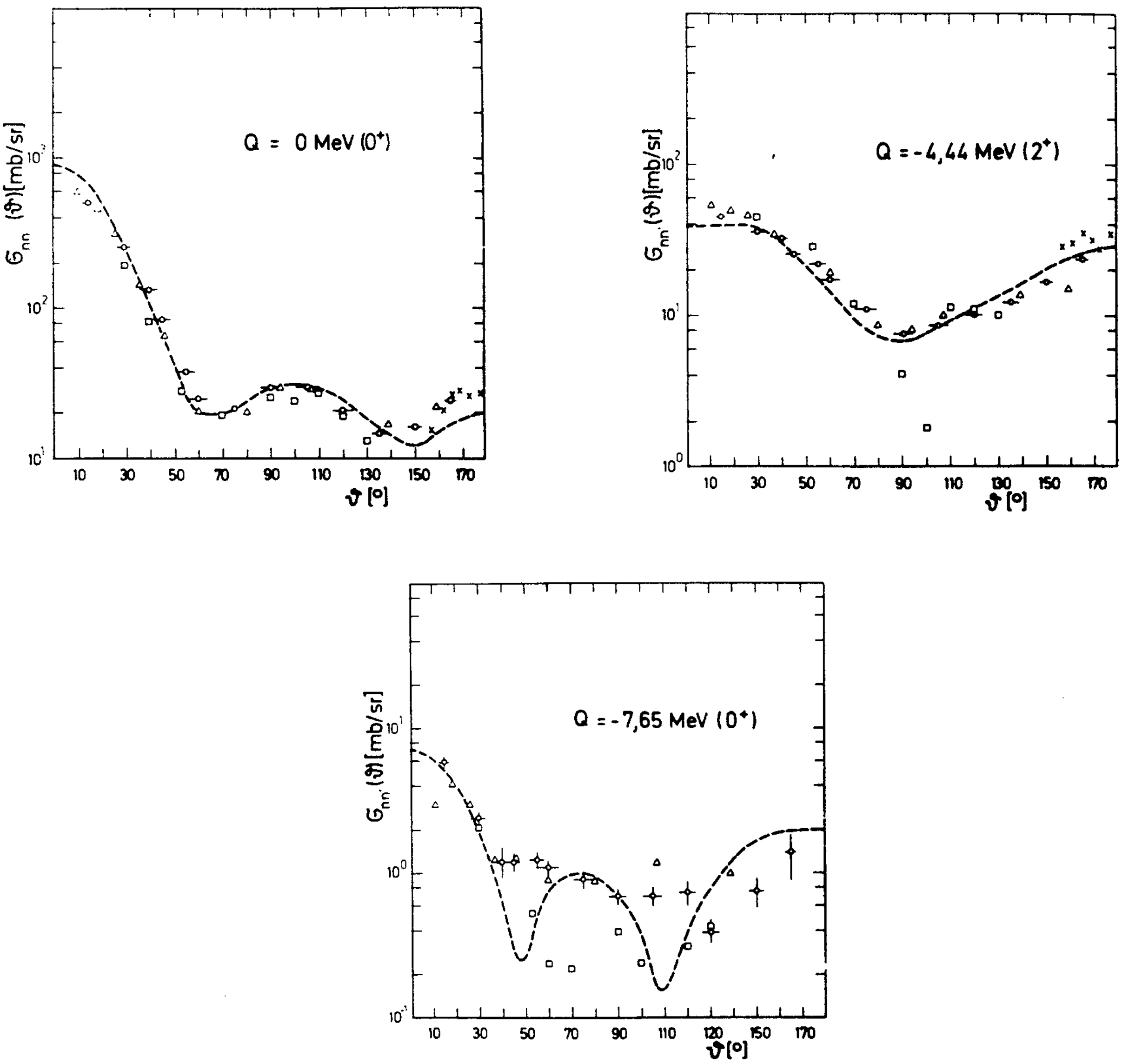

Fig. 8
Differential neutron scattering cross sections from C for the levels inserted. The experimental data of the present work (o) are compared with those from other measurements (△ ,/8/; □,/22/; x,/23/) and with the ENDF/B-V evaluation evaluation (---).

Table. 1.

Differential neutron emission cross sections from Pb in the center-of-mass system (cm)

E_o = 14.00 MeV ϑ = 15.0°

E^{cm} [MeV]	σ^{cm}_{nm} [$b \cdot sr^{-1} \cdot MeV^{-1}$]	$\Delta\sigma/\sigma$ [%]	E^{cm} [MeV]	σ^{cm}_{nm} [$b \cdot sr^{-1} \cdot MeV^{-1}$]	$\Delta\sigma/\sigma$ [%]	E^{cm} [MeV]	σ^{cm}_{nm} [$b \cdot sr^{-1} \cdot MeV^{-1}$]	$\Delta\sigma/\sigma$ [%]
2.99	.0771	27	4.78	.0215		8.92	.0147	
3.02	.0751		4.83	.0209		9.05	.0155	
3.04	.0729		4.88	.0201		9.19	.0164	
3.07	.0695		4.93	.0195		9.33	.0181	
3.09	.0666		4.99	.0190		9.47	.0188	
3.12	.0638		5.04	.0184		9.62	.0190	
3.14	.0621		5.10	.0179		9.77	.0198	
3.17	.0624		5.15	.0174		9.92	.0174	
3.20	.0627		5.21	.0170		10.08	.0139	20
3.22	.0631		5.26	.0165	29	10.24	.0083	
3.25	.0633	24	5.32	.0163		10.40	.0115	
3.28	.0632		5.38	.0159		10.57	.0173	
3.31	.0634		5.44	.0155		10.74	.0172	
3.34	.0632		5.50	.0153		10.92	.0223	
3.36	.0632		5.56	.0146		11.10	.0286	
3.39	.0631		5.63	.0147		11.29	.0297	
3.42	.0627		5.69	.0144		11.48	.0354	
3.45	.0616		5.75	.0140		11.68	.0395	
3.48	.0597		5.82	.0138		11.89	.0470	6
3.52	.0576		5.89	.0137	30	12.10	.0612	
3.55	.0558	21	5.95	.0135		12.32	.0928	
3.58	.0544		6.02	.0132		12.54	.1350	
3.61	.0527		6.09	.0131		12.77	.1871	
3.64	.0510		6.17	.0128		13.01	.3308	
3.68	.0488		6.24	.0125		13.26	.6652	
3.71	.0467		6.31	.0122		13.51	1.4537	
3.75	.0448		6.39	.0121		13.78	2.4018	
3.78	.0431		6.47	.0120		14.05	2.5044	0
3.82	.0413		6.55	.0119		14.32	2.4095	
3.85	.0395		6.63	.0118	30	14.63	1.4469	
3.89	.0378	24	6.71	.0118		14.94	.6669	
3.92	.0364		6.79	.0117		15.25	.2918	
3.96	.0352		6.88	.0118		15.58	.1845	
4.00	.0340		6.97	.0118		15.88	.1143	
4.04	.0331		7.06	.0118		16.24	.0818	
4.08	.0321		7.15	.0119		16.61	.0669	
4.12	.0314		7.24	.0121		16.98	.0541	2
4.16	.0306		7.34	.0123		17.34	.0357	
4.20	.0298		7.43	.0125		17.74	.0194	
4.24	.0292		7.53	.0128	24			
4.28	.0285	22	7.63	.0124				
4.32	.0278		7.74	.0129				
4.36	.0272		7.84	.0135				
4.41	.0266		7.95	.0136				
4.45	.0261		8.06	.0138				
4.50	.0255		8.18	.0138				
4.54	.0249		8.29	.0137				
4.59	.0243		8.41	.0136				
4.63	.0236		8.53	.0135				
4.68	.0229		8.66	.0136	22			
4.73	.0221	26	8.79	.0140				

E_0 = 14.10 MeV ϑ = 30.0°

E^{cm} [MeV]	σ^{cm}_{nm} [$b \cdot sr^{-1} \cdot MeV^{-1}$]	$\Delta\sigma/\sigma$ [%]	E^{cm} [MeV]	σ^{cm}_{nm} [$b \cdot sr^{-1} \cdot MeV^{-1}$]	$\Delta\sigma/\sigma$ [%]	E^{cm} [MeV]	σ^{cm}_{nm} [$b \cdot sr^{-1} \cdot MeV^{-1}$]	$\Delta\sigma/\sigma$ [%]
2.99	.0662	12	4.57	.0176		7.90	.0083	
3.02	.0651		4.62	.0170		8.01	.0084	
3.04	.0640		4.67	.0164	13	8.11	.0082	
3.06	.0618		4.71	.0158		8.23	.0085	
3.09	.0592		4.76	.0152		8.34	.0090	
3.11	.0569		4.81	.0147		8.46	.0088	
3.14	.0546		4.86	.0143		8.58	.0099	12
3.16	.0538		4.91	.0139		8.70	.0094	
3.19	.0535		4.96	.0135		8.82	.0084	
3.21	.0531		5.01	.0132		8.95	.0081	
3.24	.0527	10	5.07	.0128		9.08	.0065	
3.27	.0520		5.12	.0125		9.22	.0082	
3.30	.0512		5.17	.0122	15	9.35	.0091	
3.32	.0504		5.23	.0119		9.49	.0106	
3.35	.0496		5.28	.0116		9.64	.0104	10
3.38	.0490		5.34	.0114		9.79	.0088	
3.41	.0483		5.40	.0110		9.94	.0061	
3.44	.0477		5.46	.0107		10.09	.0069	
3.47	.0462		5.52	.0104		10.25	.0057	
3.50	.0445		5.58	.0101		10.41	.0039	
3.53	.0429	10	5.64	.0098		10.57	.0055	
3.56	.0416		5.70	.0095		10.74	.0056	
3.59	.0405		5.77	.0092	17	10.92	.0063	
3.62	.0394		5.83	.0089		11.09	.0078	
3.65	.0382		5.90	.0087		11.28	.0083	12
3.69	.0369		5.96	.0085		11.46	.0073	
3.72	.0356		6.03	.0083		11.66	.0064	
3.75	.0344		6.10	.0081		11.85	.0049	
3.79	.0333		6.17	.0080		12.06	.0056	
3.82	.0323		6.24	.0078		12.27	.0045	
3.86	.0314	10	6.31	.0076		12.48	.0058	
3.89	.0304		6.39	.0075		12.71	.0112	
3.93	.0296		6.46	.0074	18	12.94	.0236	
3.96	.0288		6.54	.0073		13.18	.0424	
4.00	.0282		6.62	.0072		13.42	.0870	3
4.04	.0275		6.70	.0071		13.68	.1480	
4.08	.0269		6.78	.0071		13.94	.2018	
4.11	.0261		6.86	.0070		14.21	.2138	
4.15	.0254		6.95	.0070		14.48	.1470	
4.19	.0247		7.03	.0070		14.78	.0848	
4.23	.0239	11	7.12	.0070		15.09	.0398	
4.27	.0230		7.21	.0071		15.40	.0209	
4.31	.0221		7.30	.0071	16	15.73	.0119	
4.36	.0213		7.40	.0072		16.03	.0081	
4.40	.0205		7.49	.0073		16.38	.0057	10
4.44	.0197		7.59	.0075		16.75	.0042	
4.48	.0190		7.69	.0077				
4.53	.0183		7.79	.0080				

E_o = 14.12 ϑ = 45.0°

E^{cm} [MeV]	σ^{cm}_{nm} [b·sr^{-1}·MeV^{-1}]	$\Delta\sigma/\sigma$ [%]	E^{cm} [MeV]	σ^{cm}_{nm} [b·sr^{-1}·MeV^{-1}]	$\Delta\sigma/\sigma$ [%]	E^{cm} [MeV]	σ^{cm}_{nm} [b·sr^{-1}·MeV^{-1}]	$\Delta\sigma/\sigma$ [%]
3.00	.0597	9	4.58	.0148		7.96	.0065	
3.02	.0586		4.63	.0143	11	8.07	.0065	
3.05	.0573		4.67	.0139		8.18	.0067	11
3.07	.0548		4.72	.0135		8.29	.0071	
3.10	.0519		4.76	.0131		8.40	.0073	
3.12	.0492		4.81	.0127		8.52	.0073	
3.15	.0465		4.86	.0123		8.64	.0067	
3.17	.0449		4.91	.0120		8.76	.0075	
3.20	.0439		4.96	.0116		8.89	.0062	
3.22	.0430		5.01	.0113		9.02	.0069	
3.25	.0420	10	5.06	.0110		9.15	.0088	
3.27	.0409		5.11	.0107	12	9.28	.0091	
3.30	.0397		5.17	.0104		9.42	.0080	9
3.33	.0388		5.22	.0101		9.56	.0086	
3.35	.0379		5.27	.0099		9.71	.0078	
3.38	.0374		5.33	.0096		9.85	.0073	
3.41	.0370		5.39	.0093		10.01	.0068	
3.44	.0367		5.44	.0090		10.16	.0060	
3.47	.0361		5.50	.0088		10.32	.0059	
3.50	.0352		5.56	.0085		10.48	.0059	
3.53	.0344	9	5.62	.0083		10.65	.0052	
3.56	.0336		5.68	.0080	13	10.82	.0056	
3.59	.0332		5.74	.0078		11.00	.0065	10
3.62	.0328		5.81	.0077		11.18	.0060	
3.65	.0323		5.87	.0076		11.37	.0068	
3.68	.0315		5.94	.0074		11.56	.0055	
3.71	.0307		6.01	.0074		11.75	.0049	
3.74	.0299		6.07	.0073		11.95	.0036	
3.77	.0290		6.14	.0072		12.16	.0038	
3.81	.0281		6.21	.0071		12.37	.0030	
3.84	.0271		6.29	.0070		12.59	.0086	
3.88	.0262	9	6.36	.0069		12.81	.0200	
3.91	.0252		6.44	.0068	14	13.84	.0383	3
3.94	.0242		6.51	.0066		13.28	.0872	
3.98	.0234		6.59	.0065		13.52	.1509	
4.02	.0226		6.67	.0064		13.77	.2099	
4.05	.0219		6.75	.0063		14.02	.2378	
4.09	.0212		6.83	.0062		14.30	.2479	0
4.13	.0205		6.92	.0061		14.57	.1900	
4.17	.0199	10	7.00	.0060		14.83	.0976	
4.20	.0192		7.09	.0060		15.12	.0483	
4.24	.0186		7.18	.0060	14	15.43	.0260	
4.28	.0180		7.27	.0060		15.75	.0186	3
4.32	.0174		7.36	.0060		16.05	.0135	
4.36	.0169		7.46	.0061		16.38	.0081	
4.41	.0165		7.55	.0062		16.72	.0041	
4.45	.0160		7.65	.0063		17.07	.0015	
4.49	.0156		7.75	.0064		17.41	.0007	
4.54	.0152		7.85	.0065				

E_o = 14.14 Me V ϑ= 60.0°

E^{cm} [MeV]	σ^{cm}_{nm} [$b \cdot sr^{-1} \cdot MeV^{-1}$]	$\Delta\sigma/\sigma$ [%]	E^{cm} [MeV]	σ^{cm}_{nm} [$b \cdot sr^{-1} \cdot MeV^{-1}$]	$\Delta\sigma/\sigma$ [%]	E^{cm} [MeV]	σ^{cm}_{nm} [$b \cdot sr^{-1} \cdot MeV^{-1}$]	$\Delta\sigma/\sigma$ [%]
2.99	.0574	8	4.68	.0134		8.49	.0063	
3.01	.0562		4.72	.0130		8.61	.0064	
3.04	.0549		4.77	.0126		8.73	.0063	
3.06	.0535		4.82	.0122		8.85	.0063	
3.08	.0511		4.86	.0119		8.98	.0070	
3.11	.0483		4.91	.0115		9.11	.0072	
3.13	.0456		4.96	.0112		9.24	.0073	7
3.16	.0432		5.01	.0109		9.38	.0071	
3.18	.0418		5.06	.0106	9	9.52	.0056	
3.21	.0410		5.12	.0103		9.66	.0057	
3.23	.0404	7	5.17	.0100		9.81	.0061	
3.26	.0398		5.22	.0097		9.96	.0058	
3.28	.0391		5.28	.0095		10.11	.0051	
3.31	.0383		5.33	.0092		10.27	.0052	
3.34	.0376		5.39	.0089		10.43	.0046	
3.37	.0370		5.44	.0087		10.59	.0052	
3.39	.0366		5.50	.0084		10.76	.0050	10
3.42	.0362		5.56	.0081		10.93	.0059	
3.45	.0359		5.62	.0078		11.11	.0064	
3.48	.0352		5.68	.0076	10	11.30	.0060	
3.51	.0341	7	5.74	.0073		11.48	.0060	
3.54	.0330		5.80	.0071		11.68	.0047	
3.57	.0320		5.87	.0069		11.87	.0040	
3.60	.0312		5.93	.0067		12.07	.0028	19
3.63	.0305		6.00	.0065		12.28	.0013	
3.66	.0298		6.07	.0064		12.72	.0021	
3.69	.0290		6.14	.0063		12.94	.0059	
3.72	.0281		6.21	.0061		13.18	.0152	
3.75	.0272		6.28	.0060	12	13.41	.0298	
3.78	.0265		6.35	.0059		13.66	.0432	
3.82	.0257	7	6.43	.0058		13.91	.0477	
3.85	.0250		6.50	.0058		14.18	.0534	1
3.88	.0243		6.58	.0057		14.44	.0472	
3.92	.0236		6.66	.0057		14.70	.0297	
3.95	.0229		6.74	.0056		14.99	.0142	
3.99	.0224		6.82	.0056		15.29	.0061	
4.02	.0219		6.90	.0056		15.60	.0033	
4.06	.0213		6.99	.0057		15.89	.0026	
4.10	.0207		7.08	.0057	11	16.22	.0018	11
4.14	.0202		7.16	.0058		16.55	.0015	
4.17	.0196	8	7.25	.0058		16.89	.0009	
4.21	.0190		7.35	.0058		17.23	.0004	
4.25	.0184		7.44	.0058				
4.29	.0178		7.53	.0059				
4.33	.0172		7.63	.0059				
4.37	.0166		7.73	.0062				
4.41	.0161		7.83	.0062				
4.46	.0156		7.93	.0058				
4.50	.0151		8.04	.0059	9			
4.54	.0147		8.15	.0061				
4.59	.0143	8	8.26	.0062				
4.63	.0138		8.37	.0066				

$E_0 = 14.24$ MeV $\vartheta = 75.0^\circ$

E^{cm} [MeV]	σ^{cm}_{nm} [$b \cdot sr^{-1} \cdot MeV^{-1}$]	$\Delta\sigma/\sigma$ [%]	E^{cm} [MeV]	σ^{cm}_{nm} [$b \cdot sr^{-1} \cdot MeV^{-1}$]	$\Delta\sigma/\sigma$ [%]	E^{cm} [MeV]	σ^{cm}_{nm} [$b \cdot sr^{-1} \cdot MeV^{-1}$]	$\Delta\sigma/\sigma$ [%]
3.01	.0583	11	4.61	.0143		7.93	.0049	
3.03	.0573		4.65	.0139		8.03	.0049	
3.06	.0561		4.70	.0135		8.13	.0050	
3.08	.0548		4.74	.0131		8.24	.0052	
3.11	.0521		4.79	.0127		8.34	.0052	
3.13	.0493		4.83	.0123		8.45	.0053	
3.15	.0466		4.88	.0118		8.56	.0054	
3.18	.0441		4.93	.0114		8.67	.0055	
3.20	.0430		4.98	.0109		8.79	.0055	
3.23	.0423	9	5.02	.0104	13	8.91	.0055	13
3.25	.0416		5.08	.0100		9.03	.0055	
3.28	.0410		5.13	.0096		9.15	.0061	
3.31	.0403		5.18	.0092		9.27	.0056	
3.33	.0395		5.23	.0088		9.40	.0052	
3.36	.0389		5.29	.0084		9.53	.0056	
3.39	.0383		5.34	.0081		9.67	.0057	
3.41	.0380		5.40	.0078		9.80	.0050	
3.44	.0377		5.46	.0075		9.94	.0057	
3.47	.0373		5.51	.0073		10.09	.0049	
3.50	.0365	9	5.57	.0071	16	10.23	.0056	13
3.53	.0354		5.63	.0069		10.38	.0054	
3.56	.0343		5.69	.0067		10.53	.0033	
3.59	.0331		5.76	.0065		10.68	.0038	
3.62	.0323		5.82	.0064		10.84	.0040	
3.65	.0314		5.88	.0063		11.00	.0051	
3.68	.0304		5.95	.0062		11.17	.0039	
3.71	.0293		6.01	.0061		11.33	.0038	
3.75	.0282		6.08	.0060		11.51	.0037	
3.78	.0270		6.15	.0059		11.68	.0048	
3.81	.0260	9	6.22	.0058	17	11.86	.0030	23
3.85	.0250		6.29	.0056		12.04	.0024	
3.88	.0240		6.36	.0055		12.23	.0018	
3.91	.0231		6.43	.0054		12.42	.0000	
3.95	.0222		6.50	.0053		12.62	.0000	
3.98	.0213		6.57	.0051		12.82	.0019	
4.02	.0206		6.65	.0050		13.03	.0060	
4.06	.0200		6.73	.0049		13.24	.0170	
4.09	.0194		6.80	.0048		13.46	.0296	
4.13	.0189		6.88	.0047		13.68	.0390	
4.17	.0183	11	6.96	.0047	18	13.92	.0417	
4.21	.0178		7.04	.0046		14.15	.0465	2
4.24	.0174		7.12	.0046		14.40	.0463	
4.28	.0169		7.20	.0046		14.65	.0365	
4.32	.0165		7.29	.0046		14.90	.0180	
4.36	.0161		7.38	.0046		15.18	.0070	
4.40	.0157		7.46	.0046		15.46	.0028	
4.44	.0154		7.55	.0046		15.74	.0016	
4.48	.0151		7.64	.0047		16.02	.0012	
4.52	.0148		7.74	.0047				
4.57	.0146	11	7.83	.0048	15			

$E_0 = 14.25$ MeV $\vartheta = 90.6^{\circ}$

E^{cm} [MeV]	σ^{cm}_{nm} [$b \cdot sr^{-1} \cdot MeV^{-1}$]	$\Delta\sigma/\sigma$ [%]	E^{cm} [MeV]	σ^{cm}_{nm} [$b \cdot sr^{-1} \cdot MeV^{-1}$]	$\Delta\sigma/\sigma$ [%]	E^{cm} [MeV]	σ^{cm}_{nm} [$b \cdot sr^{-1} \cdot MeV^{-1}$]	$\Delta\sigma/\sigma$ [%]
2.98	.0585	9	4.63	.0137		8.13	.0043	
3.01	.0578		4.67	.0134		8.23	.0043	
3.03	.0570		4.71	.0130		8.34	.0043	
3.05	.0560		4.76	.0127		8.45	.0044	
3.08	.0547		4.80	.0123		8.56	.0044	
3.10	.0532		4.85	.0120		8.67	.0046	
3.12	.0502		4.89	.0116		8.78	.0044	15
3.15	.0474		4.94	.0112		8.90	.0039	
3.17	.0445		4.99	.0108	12	9.02	.0040	
3.20	.0419		5.04	.0100		9.14	.0042	
3.22	.0405	9	5.09	.0100		9.27	.0051	
3.25	.0395		5.14	.0096		9.39	.0041	
3.27	.0387		5.19	.0092		9.52	.0044	
3.30	.0379		5.25	.0088		9.66	.0040	
3.32	.0370		5.30	.0085		9.79	.0044	
3.35	.0362		5.35	.0081		9.93	.0039	
3.38	.0354		5.41	.0077		10.07	.0033	19
3.40	.0348		5.47	.0074		10.21	.0033	
3.43	.0343		5.53	.0071	15	10.36	.0034	
3.46	.0339		5.58	.0068		10.51	.0029	
3.49	.0334	9	5.64	.0065		10.66	.0025	
3.52	.0325		5.71	.0062		10.82	.0029	
3.55	.0314		5.77	.0059		10.98	.0030	
3.58	.0303		5.83	.0057		11.14	.0031	
3.61	.0293		5.89	.0055		11.31	.0033	
3.64	.0286		5.96	.0053		11.48	.0037	
3.67	.0278		6.02	.0051		11.65	.0033	18
3.70	.0271		6.09	.0049		11.83	.0032	
3.73	.0263		6.16	.0048	19	12.01	.0030	
3.76	.0255		6.23	.0046		12.20	.0023	
3.80	.0248	10	6.30	.0045		12.39	.0017	
3.83	.0242		6.37	.0044		12.58	.0013	
3.86	.0236		6.44	.0043		12.78	.0011	
3.90	.0231		6.51	.0042		12.99	.0010	
3.93	.0226		6.58	.0042		13.20	.0026	
3.97	.0221		6.66	.0042		13.41	.0054	
4.00	.0215		6.73	.0042		13.63	.0095	11
4.04	.0211		6.81	.0042		13.86	.0124	
4.07	.0206		6.88	.0043	19	14.10	.0138	
4.11	.0201		6.97	.0043		14.34	.0133	
4.15	.0197	10	7.05	.0043		14.58	.0100	
4.18	.0191		7.13	.0044		14.84	.0052	17
4.22	.0185		7.21	.0044		15.10	.0031	
4.26	.0180		7.30	.0044		15.38	.0017	
4.30	.0174		7.38	.0044		15.66	.0007	
4.34	.0168		7.47	.0044		15.94	.0004	
4.38	.0162		7.56	.0044		16.24	.0004	
4.42	.0156		7.65	.0044	16	16.54	.0000	
4.46	.0152		7.74	.0044				
4.50	.0148		7.84	.0044				
4.54	.0140	11	7.93	.0044				
4.58	.0140		8.03	.0044				

E_o = 14.24 MeV ϑ = 104.5°

E^{cm} [MeV]	σ^{cm}_{nm} [$b \cdot sr^{-1} \cdot MeV^{-1}$]	$\Delta\sigma/\sigma$ [%]	E^{cm} [MeV]	σ^{cm}_{nm} [$b \cdot sr^{-1} \cdot MeV^{-1}$]	$\Delta\sigma/\sigma$ [%]	E^{cm} [MeV]	σ^{cm}_{nm} [$b \cdot sr^{-1} \cdot MeV^{-1}$]	$\Delta\sigma/\sigma$ [%]
3.00	.0557	11	4.65	.0130	11	8.15	.0041	
3.03	.0555		4.69	.0126		8.26	.0041	
3.05	.0551		4.74	.0121		8.36	.0041	
3.07	.0545		4.78	.0117		8.47	.0040	
3.10	.0536		4.82	.0113		8.58	.0039	
3.12	.0522		4.87	.0110		8.69	.0046	
3.14	.0495		4.92	.0106		8.80	.0038	19
3.17	.0470		4.97	.0103		8.92	.0031	
3.19	.0444		5.01	.0099	15	9.04	.0018	
3.22	.0420		5.06	.0096		9.16	.0038	
3.24	.0411	10	5.11	.0093		9.28	.0039	
3.27	.0401		5.16	.0089		9.41	.0037	
3.29	.0392		5.22	.0086		9.54	.0026	
3.32	.0383		5.27	.0083		9.67	.0031	
3.35	.0373		5.32	.0080		9.81	.0032	
3.37	.0364		5.38	.0077		9.95	.0025	
3.40	.0355		5.43	.0074		10.09	.0025	28
3.43	.0347		5.49	.0071		10.23	.0028	
3.45	.0341		5.55	.0068	17	10.38	.0026	
3.48	.0336		5.61	.0065		10.53	.0023	
3.51	.0330	11	5.67	.0063		10.68	.0015	
3.54	.0320		5.73	.0060		10.84	.0010	
3.57	.0309		5.79	.0057		10.99	.0017	
3.60	.0299		5.85	.0055		11.16	.0029	
3.63	.0289		5.92	.0053		11.32	.0023	
3.66	.0282		5.98	.0051		11.49	.0024	
3.69	.0275		6.05	.0050		11.66	.0016	40
3.72	.0267		6.11	.0048		11.84	.0025	
3.75	.0259		6.18	.0046	21	12.02	.0019	
3.78	.0250		6.25	.0045		12.21	.0007	
3.82	.0242	11	6.32	.0043		12.40	.0010	
3.85	.0235		6.39	.0042		12.59	.0006	
3.88	.0228		6.46	.0040		12.79	.0000	
3.92	.0221		6.53	.0039		12.99	.0037	
3.95	.0215		6.61	.0039		13.20	.0054	20
3.99	.0209		6.68	.0038		13.42	.0107	
4.02	.0203		6.76	.0038		13.64	.0127	
4.06	.0198		6.83	.0038		13.86	.0145	
4.10	.0194		6.91	.0038	23	14.10	.0155	
4.13	.0190		6.99	.0038		14.34	.0148	
4.17	.0186	11	7.07	.0038		14.58	.0129	
4.21	.0181		7.15	.0038		14.84	.0109	
4.24	.0177		7.23	.0039		15.10	.0045	14
4.28	.0172		7.32	.0039		15.37	.0013	
4.32	.0168		7.40	.0040		15.65	.0006	
4.36	.0162		7.49	.0040		15.94	.0005	
4.40	.0157		7.58	.0041				
4.44	.0152		7.67	.0041				
4.48	.0147		7.76	.0041	19			
4.52	.0143		7.86	.0042				
4.56	.0138		7.95	.0043				
4.61	.0134		8.05	.0042				

E_o = 14.12 MeV ϑ = 120.0 °

E^{cm} [MeV]	σ^{cm}_{nm} [$b \cdot sr^{-1} \cdot MeV^{-1}$]	$\Delta\sigma/\sigma$ [%]	E^{cm} [MeV]	σ^{cm}_{nm} [$b \cdot sr^{-1} \cdot MeV^{-1}$]	$\Delta\sigma/\sigma$ [%]	E^{cm} [MeV]	σ^{cm}_{nm} [$b \cdot sr^{-1} \cdot MeV^{-1}$]	$\Delta\sigma/\sigma$ [%]
2.98	.0564	8	4.62	.0117	10	8.17	.0028	
3.01	.0552		4.66	.0114		8.28	.0029	
3.03	.0540		4.71	.0110		8.39	.0029	
3.05	.0531		4.75	.0106		8.50	.0029	
3.08	.0522		4.80	.0102		8.61	.0030	
3.10	.0512		4.84	.0098		8.73	.0030	
3.12	.0500		4.89	.0094		8.85	.0032	14
3.15	.0481		4.94	.0090		8.97	.0034	
3.17	.0457		4.99	.0086	11	9.10	.0031	
3.19	.0433		5.04	.0082		9.23	.0028	
3.22	.0410	7	5.09	.0079		9.36	.0028	
3.24	.0395		5.14	.0075		9.49	.0024	
3.27	.0386		5.19	.0072		9.63	.0022	
3.29	.0377		5.24	.0069		9.77	.0021	
3.32	.0367		5.30	.0067		9.92	.0020	
3.35	.0357		5.35	.0064		10.06	.0021	
3.37	.0346		5.41	.0062		10.21	.0010	25
3.40	.0335		5.47	.0060		10.37	.0014	
3.43	.0325		5.52	.0058	13	10.52	.0009	
3.46	.0316		5.58	.0056		10.69	.0014	
3.48	.0309	8	5.64	.0054		10.85	.0012	
3.51	.0303		5.70	.0053		11.02	.0012	
3.54	.0295		5.76	.0051		11.19	.0010	
3.57	.0285		5.82	.0049		11.37	.0019	
3.60	.0276		5.89	.0048		11.55	.0016	
3.63	.0267		5.95	.0046		11.74	.0012	35
3.66	.0261		6.01	.0044		11.93	.0004	
3.69	.0257		6.08	.0043		12.12	.0007	
3.72	.0253		6.15	.0041	17	12.32	.0010	
3.75	.0247		6.21	.0040		12.53	.0011	
3.79	.0241	8	6.28	.0039		12.75	.0015	
3.82	.0235		6.35	.0038		12.97	.0017	
3.85	.0229		6.42	.0036		13.19	.0037	
3.89	.0223		6.50	.0036		13.42	.0055	
3.92	.0216		6.57	.0035		13.66	.0068	
3.95	.0208		6.65	.0034		13.92	.0066	
3.99	.0201		6.72	.0034		14.17	.0065	11
4.02	.0193		6.80	.0034		14.44	.0045	
4.06	.0186		6.88	.0034	17	14.71	.0037	
4.10	.0179		6.96	.0034		15.00	.0030	
4.13	.0173	8	7.04	.0034		15.27	.0029	
4.17	.0166		7.13	.0034		15.59	.0014	
4.21	.0160		7.21	.0034		15.91	.0010	33
4.25	.0154		7.30	.0033		16.24	.0005	
4.29	.0149		7.39	.0033		16.58	.0004	
4.33	.0144		7.48	.0033		16.89	.0006	
4.37	.0139		7.57	.0032				
4.41	.0134		7.67	.0030				
4.45	.0130		7.76	.0029	17			
4.49	.0127		7.86	.0031				
4.53	.0124		7.96	.0032				
4.57	.0120		8.07	.0031				

E_o = 14.12 MeV ϑ = 135.0 °

E^{cm} [MeV]	σ^{cm}_{nm} [$b \cdot sr^{-1} \cdot MeV^{-1}$]	$\Delta\sigma/\sigma$ [%]	E^{cm} [MeV]	σ^{cm}_{nm} [$b \cdot sr^{-1} \cdot MeV^{-1}$]	$\Delta\sigma/\sigma$ [%]	E^{cm} [MeV]	σ^{cm}_{nm} [$b \cdot sr^{-1} \cdot MeV^{-1}$]	$\Delta\sigma/\sigma$ [%]
3.00	.0550	10	4.55	.0121		7.86	.0032	
3.02	.0536		4.59	.0117		7.96	.0032	
3.04	.0521		4.63	.0112		8.06	.0032	
3.06	.0510		4.68	.0108		8.17	.0033	
3.09	.0498		4.72	.0104		8.27	.0033	
3.11	.0487		4.77	.0100		8.38	.0033	
3.13	.0474		4.81	.0096		8.50	.0033	
3.16	.0457		4.86	.0093		8.61	.0033	
3.18	.0435		4.91	.0089		8.73	.0032	19
3.20	.0414		4.95	.0086	15	8.85	.0031	
3.23	.0395	10	5.00	.0083		8.97	.0031	
3.25	.0381		5.05	.0081		9.09	.0030	
3.28	.0377		5.10	.0078		9.22	.0029	
3.30	.0373		5.15	.0076		9.35	.0028	
3.33	.0369		5.20	.0074		9.48	.0026	
3.35	.0364		5.25	.0072		9.62	.0025	
3.38	.0357		5.31	.0069		9.76	.0023	
3.41	.0350		5.36	.0067		9.91	.0022	
3.43	.0342		5.42	.0065		10.05	.0020	29
3.46	.0336		5.47	.0062	18	10.20	.0019	
3.49	.0330	9	5.53	.0060		10.36	.0018	
3.52	.0323		5.58	.0057		10.52	.0016	
3.55	.0317		5.64	.0055		10.68	.0013	
3.57	.0305		5.70	.0053		10.84	.0012	
3.60	.0293		5.76	.0050		11.01	.0012	
3.63	.0281		5.82	.0048		11.19	.0012	
3.66	.0271		5.88	.0045		11.37	.0012	
3.69	.0263		5.94	.0043		11.55	.0012	
3.72	.0255		6.01	.0041		11.74	.0010	52
3.75	.0248		6.07	.0039	24	11.93	.0008	
3.78	.0239	10	6.14	.0037		12.13	.0007	
3.82	.0231		6.21	.0035		12.33	.0007	
3.85	.0222		6.28	.0034		12.54	.0009	
3.88	.0215		6.35	.0032		12.75	.0014	
3.91	.0208		6.42	.0030		12.97	.0024	
3.95	.0202		6.49	.0029		13.20	.0036	22
3.98	.0195		6.57	.0028		13.43	.0049	
4.02	.0189		6.64	.0027		13.68	.0065	
4.05	.0183		6.72	.0026		13.91	.0071	
4.08	.0179		6.80	.0025	31	14.16	.0073	13
4.12	.0174	11	6.88	.0025		14.42	.0065	
4.16	.0169		6.96	.0025		14.70	.0059	
4.19	.0165		7.04	.0025		14.97	.0046	
4.23	.0160		7.12	.0026		15.23	.0028	33
4.27	.0156		7.21	.0026		15.53	.0014	
4.31	.0151		7.30	.0027		15.84	.0004	
4.34	.0146		7.39	.0028				
4.38	.0141		7.48	.0029				
4.42	.0136		7.57	.0029				
4.46	.0130		7.67	.0030	22			
4.51	.0126	12	7.76	.0031				

E_o = 14.10 MeV ϑ = 150.0°

E^{cm} [MeV]	σ^{cm}_{nm} [b·sr^{-1}·MeV^{-1}]	$\Delta\sigma/\sigma$ [%]	E^{cm} [MeV]	σ^{cm}_{nm} [b·sr^{-1}·MeV^{-1}]	$\Delta\sigma/\sigma$ [%]	E^{cm} [MeV]	σ^{cm}_{nm} [b·sr^{-1}·MeV^{-1}]	$\Delta\sigma/\sigma$ [%]
3.01	.0662	13	4.62	.0125		8.08	.0024	
3.03	.0642		4.66	.0121		8.19	.0024	
3.05	.0621		4.71	.0117		8.29	.0024	
3.08	.0603		4.75	.0112		8.40	.0023	
3.10	.0584		4.80	.0107		8.51	.0023	
3.12	.0565		4.84	.0102		8.63	.0023	46
3.15	.0546		4.89	.0097		8.74	.0022	
3.17	.0519		4.94	.0092	24	8.86	.0022	
3.19	.0487		4.98	.0087		8.98	.0021	
3.22	.0458	14	5.03	.0082		9.10	.0020	
3.24	.0431		5.08	.0078		9.23	.0019	
3.27	.0412		5.13	.0074		9.36	.0017	
3.29	.0401		5.18	.0070		9.49	.0015	
3.32	.0391		5.24	.0066		9.62	.0016	
3.34	.0382		5.29	.0063		9.76	.0013	
3.37	.0372		5.34	.0061		9.90	.0011	
3.39	.0363		5.40	.0058		10.05	.0010	90
3.42	.0354		5.45	.0056	33	10.20	.0009	
3.45	.0346		5.51	.0053		10.35	.0007	
3.48	.0341	15	5.57	.0051		10.50	.0006	
3.50	.0337		5.62	.0049		10.66	.0006	
3.53	.0333		5.68	.0047		10.82	.0008	
3.56	.0329		5.74	.0045		10.99	.0014	
3.59	.0319		5.80	.0043		11.16	.0016	
3.62	.0309		5.86	.0041		11.33	.0018	
3.65	.0299		5.93	.0040		11.51	.0013	55
3.68	.0290		5.99	.0038		11.69	.0009	
3.71	.0283		6.05	.0036	42	11.87	.0004	
3.74	.0275		6.12	.0035		12.07	.0002	
3.77	.0266	15	6.19	.0033		12.26	.0008	
3.80	.0255		6.25	.0032		12.46	.0012	100
3.83	.0244		6.32	.0031		12.67	.0013	
3.87	.0234		6.39	.0029		12.89	.0025	
3.90	.0224		6.46	.0029		13.11	.0050	
3.93	.0214		6.53	.0028		13.33	.0062	
3.97	.0205		6.61	.0028		13.57	.0073	
4.00	.0196		6.68	.0027		13.81	.0079	20
4.04	.0188		6.76	.0027	49	14.06	.0064	
4.07	.0180		6.83	.0027		14.31	.0040	
4.11	.0174	18	6.91	.0027		14.58	.0019	
4.14	.0169		6.99	.0027		14.85	.0017	
4.18	.0164		7.07	.0027		15.14	.0027	
4.22	.0160		7.16	.0027		15.42	.0029	42
4.26	.0156		7.24	.0027		15.73	.0027	
4.29	.0152		7.33	.0027		16.05	.0020	
4.33	.0149		7.42	.0026		16.38	.0010	
4.37	.0145		7.51	.0026		16.72	.0006	
4.41	.0142		7.60	.0026	45			
4.45	.0138		7.69	.0025				
4.49	.0135	19	7.79	.0025				
4.54	.0132		7.88	.0025				
4.58	.0128		7.98	.0024				

Tab. 2. Angular distributions of neutrons elastically and inelastically scattered from C in the center-of-mass system (cm).

E_o [MeV]	ϑ [°]	ϑ^{cm} [°]	$\sigma^{cm}_{nn} \pm \Delta\sigma$ [$mb \cdot sr^{-1}$]	ϑ^{cm} [°]	$\sigma^{cm}_{nn'} \pm \Delta\sigma$ [$mb \cdot sr^{-1}$]	ϑ^{cm} [°]	$\sigma^{cm}_{nn'} \pm \Delta\sigma$ [$mb \cdot sr^{-1}$]
		Q = 0		Q = -4,439 MeV		Q = -7,653 MeV	
14.08	15.0	16.2	430.6 ± 1.2	16.5	37.3 ± 0.5	16.9	4.6 ± 0.3
14.10	30.0	32.4	224.5 ± 0.8	32.9	30.0 ± 0.2	33.7	1.9 ± 0.1
14.11	40.3	43.4	118.1 ± 0.6	44.1	27.3 ± 0.3	45.1	1.0 ± 0.3
14.11	45.0	48.4	74.8 ± 0.3	49.2	22.4 ± 0.2	50.3	1.0 ± 0.2
14.12	55.6	59.5	33.7 ± 0.4	60.4	19.5 ± 0.3	61.7	1.1 ± 0.1
14.12	60.0	64.1	22.6 ± 0.2	65.1	15.7 ± 0.2	66.4	0.97 ± 0.1
14.24	75.0	79.6	20.1 ± 0.2	80.7	10.3 ± 0.1	82.2	0.85 ± 0.1
14.25	90.6	95.4	29.3 ± 0.2	96.5	7.5 ± 0.1	98.0	0.69 ± 0.1
14.24	104.5	109.1	30.4 ± 0.3	110.2	8.9 ± 0.1	111.7	0.75 ± 0.1
14.12	120.0	124.1	22.2 ± 0.3	125.1	11.3 ± 0.1	126.4	0.84 ± 0.2
14.11	135.0	138.4	15.7 ± 0.2	139.2	14.2 ± 0.2	140.3	0.46 ± 0.1
14.10	150.0	152.4	17.9 ± 0.5	152.9	19.9 ± 0.3	153.7	0.94 ± 0.2
14.08	165.0	166.2	27.1 ± 1.3	166.5	28.5 ± 0.7	166.9	1.8 ± 0.6

References

/ 1/ International Tokamak Reactor, IAEA STI/PUB/619, Vienna 1982, p. 450-476.
/ 2/ World Request List for Nuclear Data, INDC(SEC)-88/URSF, IAEA Vienna, 1983.
/ 3/ P.M. Schetman and J.D. Anderson, Nucl. Phys. 77(1966) 241.
/ 4/ G. Clayeux and J. Voigner, CEAR 4279(1972).
/ 5/ J.L. Kammerdiener, Thesis Ph.D., UCRL-51232(1972).
/ 6/ D. Hermsdorf et al., ZfK-277(U)(1975), INDC(GDR)-2/L.
/ 7/ H. Vonach et al., BNL-NCS-51245, INDC(USA)-84/L(1980).
/ 8/ A. Takahashi et al., Oktavian-Report A-83-01(1983).
/ 9/ H. Helfer et al., INDC(GDR)-34/GI, IAEA Vienna 1985, p.13.
/ 10/ R. Arlt et al., ZfK-408(1979) 154.
/ 11/ M. Adel-Fawzy et al., ZfK-408(1979) 150.
/ 12/ D. Hermsdorf, ZfK-315(1976) 192.
/ 13/ T. Elfruth et al., INDC(GDR)-34/GI,IAEA Vienna 1985, p.11
/ 14/ L. Rodrigues, Forschungspraktikum, TU Dresden, 1985.
/ 15/ M.B. Emmet, ORNL-4972(1975).
/ 16/ F.G. Percey, ENDF/B-IV, Library, MAT 1288.
/ 17/ H.D. Giera et al., Kernenergie 14(1971) 115.
/ 18/ K. Nakagama et al., Nucl. Instr. Meth. 190(1981) 555.
/ 19/ A.I. Ignatyuk, V.P. Lunev, private comm., 1983.
/ 20/ H. Kalka, Diplomarbeit, TU Dresden, 1983.
/ 21/ M. Uhl, B. Strohmaier, IRK-76/1, 1976.
/ 22/ K. Guhl et al., Phys. Rev. 24(1981) 2458.
/ 23/ C. Bonazzola et al., Lettre al Nuovo Cimento 3(1972) 99.